Received: 3 August 2021 | Revised: 17 February 2022 | Accepted: 17 May 2022

DOI: 10.1002/ajpa.24569

BRIEF COMMUNICATION

AMERICAN JOURNAL OF BIOLOGICAL ANTHROPOLOGY
The Official Journal of the American Association of Biological Anthropologists

WILEY

A structural reassessment of the Late Pleistocene femur from Maludong, southwestern China

Pianpian Wei[1,2,3] | Shiwu Ma[4] | Kristian J. Carlson[5,6] | Xueping Ji[7,8] | Quanchao Zhang[9] | Wu Liu[10,11] | Li Jin[12,13]

[1]Department of Cultural Heritage and Museology, Fudan University, Shanghai, China

[2]Institute of Archaeological Science, Fudan University, Shanghai, China

[3]Centre for the Exploration of the Deep Human Journey, Faculty of Science, University of the Witwatersrand, Johannesburg, South Africa

[4]Mengzi Institute of Cultural Relics, Mengzi, Yunnan, China

[5]Department of Integrative Anatomical Sciences, Keck School of Medicine, University of Southern California, Los Angeles, California, USA

[6]Evolutionary Studies Institute, University of the Witwatersrand, Johannesburg, South Africa

[7]Kunming Natural History Museum of Zoology, Kunming Institute of Zoology, Chinese Academy of Sciences, Kunming, China

[8]Yunnan Institute of Cultural Relics and Archaeology, Kunming, Yunnan, China

[9]Department of Archaeology, Jilin University, Changchun, China

[10]Key Laboratory of Vertebrate Evolution and Human Origins, Institute of Vertebrate Palaeontology and Palaeoanthropology, Chinese Academy of Sciences, Beijing, China

[11]CAS Center for Excellence in Life and Paleoenvironment, Beijing, China

[12]State Key Laboratory of Genetic Engineering, Collaborative Innovation Center for Genetics and Development, School of Life Sciences, Fudan University, Shanghai, China

[13]Human Phoneme Institute, Fudan University, Shanghai, China

Correspondence
Pianpian Wei, Department of Cultural Heritage and Museology, Fudan University, Shanghai, 200438, China.
Email: weipianpian@fudan.edu.cn

Kristian J. Carlson, Department of Integrative Anatomical Sciences, Keck School of Medicine, University of Southern California, Los Angeles, California 90033, USA.
Email: kristian.carlson@usc.edu

Funding information
111 Project, Grant/Award Number: B13016; China Postdoctoral Science Foundation, Grant/Award Number: 2017M611449; Key projects of strategic international scientific and technological innovation cooperation of the Chinese Ministry of Science and Technology, Grant/Award Number: 2020YFE0201600; National Natural Science Foundation of China, Grant/Award Number: 41802020; Scientific and Technology Committee of Shanghai Municipality, Grant/Award Number: 18490750300; Strategic Priority Research Program of the Chinese Academy of Sciences, Grant/Award Number: XDB26000000

Abstract

Objective: The Late Pleistocene partial right femur from Maludong in southwestern China has been attributed characteristics of early *Homo*, especially from the Early Pleistocene, putatively representing a late surviving archaic population in the region. Assessment of additional traits is warranted given newly described postcrania from the Late Pleistocene of southwestern China and characterized by relatively modern features.

Materials and methods: We used micro computed tomography (μCT) to extract and evaluate cross-sectional diaphyseal structure. New predictions of Maludong femoral length were generated from a regression analysis of Holocene modern humans. Robusticity and shape at multiple, standard diaphyseal regions of interest (ROI) were compared to those of Pleistocene and Holocene humans from East Asia and beyond.

Results: Standardized torsional rigidities at mid-proximal and subtrochanteric Maludong ROIs fell within ranges of variation exhibited by multiple comparative groups, and closest to medians of Early and Middle Upper Paleolithic modern humans (E/MUP). For I_x/I_y diaphyseal ratios, Maludong was higher than comparative groups at both ROIs, falling closest to the upper end of the E/MUP range. For I_{max}/I_{min} shape ratios, Maludong fell well above group medians at the mid-proximal ROI and nearest E/MUP and Middle Pleistocene group medians at the subtrochanteric ROI.

Discussion and conclusions: In diaphyseal robusticity and rigidity ratios, Maludong fits within variation exhibited by other Late Pleistocene modern humans. While we did not re-analyze external features described as archaic-like, internal structure of the Maludong femur contradicts this characterization and instead supports expanding intrapopulation variability expressed by Late Pleistocene modern humans in East Asia.

KEYWORDS
cross-sectional geometry, East Asia, femoral diaphysis, modern humans

1 | INTRODUCTION

Femoral remains from the Late Pleistocene of East Asia are rare, which is unfortunate given the primary importance of this skeletal element for documenting activity patterns in past human groups (Carlson & Marchi, 2014; Ruff et al., 1984; Ruff, Holt, et al., 2015; Stock & Macintosh, 2016; Stock & Pfeiffer, 2004). Those examples with relatively accurate chronological dating include femora from Tianyuan 1, Maomaodong and Maludong. The Tianyuan 1 femora are relatively complete and exhibit distinct pilasters, which clearly resemble the form of those of early modern humans (Shang & Trinkaus, 2010; Wei et al., 2017; Wei, Zhao, et al., 2021). Although two of the Maomaodong partial femora also exhibit distinct pilasters, their form and the weakly developed pilaster on a third Maomaodong partial femur expand the range of intragroup femoral variation observed in East Asia (Wei, Weng, et al., 2021). External morphology and dimensions of the Maludong partial femur (i.e., a long biomechanical neck length, a posteriorly oriented lesser trochanter, pronounced medial buttressing, a marked gluteal buttress, low neck-shaft angle, and a weakly developed pilaster) have been used to highlight its archaic-like features (Curnoe et al., 2015), but unlike the other Late Pleistocene femora from this region, systematic internal investigation of the Maludong femur has not yet been undertaken.

Here we provide the initial analyses of shaft robusticity, rigidity, and shape for the Maludong partial femur. Cross-sectional geometric (CSG) analyses of femoral diaphyses produce useful insights into body shape and activity patterns, as well as taxonomic relationships (e.g., Puymerail et al., 2012; Ruff, 2009; Ruff, Holt, Sládek, et al. (2006); Ruff, Holt, and Trinkaus (2006); Shackelford, 2007; Trinkaus & Ruff, 1999; Wei et al., 2017; Wei, Weng, et al., 2021), although they are not always straightforward reflections of form-function relationships (e.g., see Ruff, Holt, Sládek, et al., 2006; Ruff, Holt, & Trinkaus, 2006). Nonetheless, in order to have a more comprehensive morphological understanding of the Maludong femur and contextualize its comparability to contemporary femora from the broader East Asia region, we produce new estimates of its length with a regression-based analysis and undertake a systematic internal structural analysis at selected diaphyseal locations. Specifically, we calculate CSGs from two regions of interest (ROIs) that is, 65% and 80% of biomechanical length, and compare them to those of other early humans from East Asia and other regions more broadly speaking, including the Early, Middle, and Late Pleistocene of Eurasia and Africa.

We use comparisons in this study to evaluate whether the Maludong femur is structurally more similar to those of early *Homo* or modern humans. If the Maludong partial femur exhibits early *Homo*-like features in its internal structure, seemingly corroborating selected aspects of its external morphology (see Curnoe et al., 2015), we predict that the Maludong partial femur will be distinguishable from contemporary East Asian humans that exhibit modern human-like features (i.e., Tianyuan 1 and Maomaodong femora). If, however, the Maludong femur is not internally distinctive from contemporary East Asian humans (i.e., Tianyuan 1 and Maomaodong femora), then this would suggest that the Maludong partial femur might simply represent an expanded range of intragroup variability in femoral morphology of the region, especially externally, rather than representing a separate and distinct, archaic-like population. Structural similarities or differences between the Maludong femur and contemporary femora from East Asia ultimately could benefit comparative assessments of the activity patterns of these individuals (e.g., mobility levels).

2 | MATERIALS AND METHODS

2.1 | Materials

Maludong is located at the edge of Huangjia mountain, Hongzhai village, near Mengzi city, Honghe Prefecture, Yunnan province, southwestern China (23°20′N, 103°24′E) (Zhang et al., 1990). The site was originally excavated in 1989. Remains from at least five individuals were recovered and described, including craniodental and postcranial elements (Zhang et al., 1990). All human fossils were recovered from a portion of the deposit dated with Accelerator Mass Spectrometry (AMS) (^{14}C charcoal) between 14,310 ± 340 and 13,590 ± 160 cal. year BP.

The Maludong partial femur (MLDG 1678, Figure 1) is stored at the Mengzi Institute of Cultural Relics, Mengzi, Yunnan Province, China. It is 175 mm long and retains much of the proximal diaphysis from a right femur (Curnoe et al., 2015). Previous study suggested its midshaft was present and a "region for midshaft (MS) measurements

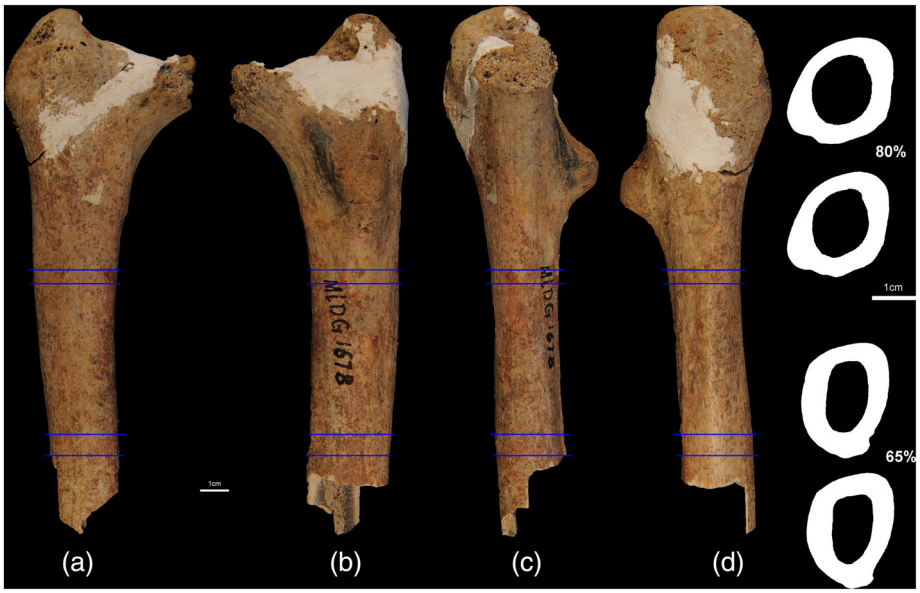

FIGURE 1 The Maludong right femur, MLDG 1678. (a) Anterior view; (b) posterior view; (c) medial view; (d) lateral view. Blue lines indicate locations of 65% and 80% regions of interest (ROIs) used in the study. The range at each ROI reflects estimated length ± average error estimate

TABLE 1 Comparative Pleistocene samples[a] in structural analyses.

Region of interest	Group	Specimens
65%	EP	KNM-ER 736, 737, 803a, 1472, 1481a, 1808mn, Kresna 11
	EMP	Aïn Maarouf 1, AT-SH F-X, XI, XIII, XVI, AT-1020, Gesher-B.-Y. 1, OH 28, Trinil II, III, IV
	LMP	Broken Hill E690, Tabun E1, Karain
	NEA	Amud 1, CDV-Tour 1, Feldhofer 1, Ferrassie 1, 2, Fond-de-Forêt 1, Krapina 257.32, 257.33, Palomas 52, 92, 96, Quina 38, Shanidar 6, Spy 2
	MPMH (LPMH)	Qafzeh 6, 8, 9, Skhul 4, 5
	EUP/MUP (LPMH)	Cro-Magnon 1, 4322, 4324, Dolní Věstonice 3, 13, 14, 16, 41, Eiv Gev 1, Minatogawa 1, 3, 4, Mladeč 27, 28, Nahal 'En-Gev 1, Ohalo 2, Paviland, Pavlov 1, Sunghir 1, 4, Tianyuan 1, Willendorf 1
	LUP (East Asia, LPMH)	GM7506, GM7508
80%	EP	KNM-ER 736, 737, 803a, 1472, 1481a, 1808mn, Kresna 11
	EMP	AT-SH F-X, XI, XIII, XIV, XVI, AT-1020, Gesher-B.–Y. 1, OH 28, Trinil II, III, IV
	LMP	Broken Hill E689, E690, E709, La Chaise-BD 5, Tabun E1
	NEA	Amud 1, Chapelle-aux-Saints 1, Feldhofer 1, Ferrassie 1, 2, Krapina 213, 214, Saint-Césaire 1, Spy 2, Tabun 1
	MPMH (LPMH)	Qafzeh 8, 9, Skhul 4, 5, 6, 9
	EUP/MUP (LPMH)	Arene Candide 1, Barma Grande 2, Cro-Magnon 1, 4322, Dolní Věstonice 3, 13, 14, 16, 35, Ein Gev 1, Grotte-des-Enfants 4, Minatogawa 1, 2, 3, 4, Mladeč 27, 28, Nahal 'En-Gev 1, Ohalo 2, Paglicci 25, Paviland 1, Pavlov 1, Rochette 2, Sunghir 1,Tianyuan 1, Veneri 1, 2
	LUP (East Asia, LPMH)	GM7508

Note: Chevalier et al. (2015); Puymerail et al. (2012); Rodríguez et al. (2018); Ruff, Puymerail, et al. (2015)
Abbreviations: EMP, Early middle Pleistocene (400,000–780.000 BP); EP, Early Pleistocene (>780,000 BP); EUP/MUP, Early Upper Paleolithic/Middle Upper Paleolithic modern humans; LMP, Late Middle Pleistocene (126,000–400,000 BP); LUP, Late Upper Paleolithic modern humans; MPMH, Middle Paleolithic modern humans; NEA, Neandertals; LPMH, Late Pleistocene modern humans (11,700–126,000 BP).
[a]Comparative data of specimens originated mainly from Trinkaus and Ruff (2012), while specimen data published after 2012 come from several sources, i.e., Kresna 11 from Puymerail et al. (2012), AT-SH-F-X, XI, XIII, XIV, XVI, AT-1020 from Rodríguez et al. (2018), Trinil II, III, IV from Ruff, Puymerail, et al. (2015); and Karain from Chevalier et al. (2015).

was selected following identification of a pilaster" on the incomplete specimen (Curnoe et al., 2015). Descriptive morphology of the external surface of MLDG 1678 has been published by Curnoe et al. (2015), so the current study focuses on quantifying complementary features such as internal CSG properties of the diaphysis and a new regression-based estimation of its biomechanical length.

In order to broadly evaluate MLDG 1678 CSG properties, we compared them to those of other Pleistocene hominins. Specifically, we used a comparative sample partitioned into six groups from Eurasia and Africa following an approach used mainly by Trinkaus and Ruff (2012) and also others (Chevalier et al., 2015; Puymerail et al., 2012; Rodríguez et al., 2018; Ruff, Puymerail, et al., 2015) (Table 1): Early Pleistocene (EP,

>780,000 BP), early Middle Pleistocene (EMP, 400,000–780,000 BP), late Middle Pleistocene (LMP, 126,000–400,000 BP), late archaic *Homo* (Neandertals, NEA), Middle Paleolithic modern humans (MPMH), Early and Middle Upper Paleolithic modern humans (E/MUP), and Late Upper Paleolithic modern humans. The latter group includes only the two East Asian Maomaodong femora (GM7506 and GM7508).

In order to estimate biomechanical length of the Maludong partial femur, Holocene recent modern human samples from China, encompassing a total of 59 adult individuals, were selected for comparison (Table 2). Adult determination was made by selecting individuals exhibiting complete fusion of femoral epiphyses. Archeological groups comprising this Holocene sample included the Tuchengzi population (HT, $n = 25$), which is from the late Warring States period during the end of the 3rd century BC in Helingeer county, Inner Mongolia, northern China; the Xindianzi population (HX, $n = 5$), which is from the middle of the Spring and Autumn period to the early Warring States period during the 6th to 5th century BC in Helingeer county, Inner Mongolia, northern China; and the Jinggouzi population (LJ, $n = 21$), which is from the late Spring and Autumn period to the early Warring States period during the 5th century BC in Linxi county, Inner Mongolia, northern China. We also included an Early 20th century modern human population (MH, n = 8), which is from the Second World War in Yunnan province, southern China.

2.2 | CT data collections

The Maludong femur (MLDG 1678) was scanned using the 450 kV industrial high resolution computed tomography system developed by the Institute of High Energy Physics, Chinese Academy of Sciences (CAS) at the Key Laboratory of Vertebrate Evolution and Human Origins. The specimen was scanned with a beam energy of 360 kV and a flux of 1.5 mA at a resolution of 160 μm per pixel using a 360° rotation with a step size of 0.25°. A total of 1440 projections were reconstructed in a 2048 × 2048 matrix of 2048 slices using two-dimensional reconstruction software developed by the Institute of High Energy Physics, CAS (Wang et al., 2019).

2.3 | Biomechanical length estimation

We derived an estimate of biomechanical length of MLDG 1678, in part, to select locations of specific cross sections of interest for structural analyses, e.g., 50% and 80% of biomechanical length. In our analyses, the distalmost location of the femur is defined as 0% diaphyseal length.

All modern human femora used in the length estimation procedure were surface scanned using a laser scanner (RANGE 7: accuracy ±40 μm, density resolution 80 μm) and measured in a standardized posterior view using 3-matic (Materialize's interactive medical image control system). In order to ensure repeatability, all landmarks selected for femoral biomechanical length estimation were basic anatomical sites that were present on the comparative modern human and Maludong femora. Landmarks defining the measurements are described in Table 3. Three landmarks (F1, F3, and F5) follow those defined by Steele (1970) and Wright and Vásquez (2003). Considering preservation of MLDG 1678, we used two additional landmarks to produce a more secure regression equation for the biomechanical length estimation that is, superior surface of the neck at its deepest (most distal) point (F2), and superoinferior midpoint of the gluteal tuberosity (F4) (see Table 3). All measurements were recorded in millimeters (Table 4). Summary statistics for segment lengths and

TABLE 2 Sample for femur length regression analysis.

	Male		Female		
Locality of modern human samples	Right	Left	Right	Left	Total
Tuchengzi	11	10	1	3	25
Xindianzi	3	2	–	–	5
Jinggouzi	8	5	5	3	21
Early 20th century modern human	2	–	6	–	8
Total	24	17	12	6	59

TABLE 3 Definitions of landmarks used in estimating femoral length.

Landmark	Landmark[a]	Landmark[b]	Definition
F1	1		Most proximal point on the greater trochanter
F2			Superior surface of the neck at its deepest (most distal) point
F3	2	2	Superoinferior midpoint of the lesser trochanter
F4			Superoinferior midpoint of the gluteal tuberosity
F5	3		Point on the shaft immediately proximal to the intersection of the pectineal line and the linea aspera

[a]From Wright and Vásquez (2003).
[b]From Steele (1970).

TABLE 4 Segment lengths between sets of landmarks and biomechanical length (BL) measurements for archeological specimens.

Specimen no.	Sex	Side	F1–F3[a]	F1–F4	F1–F5	F2–F3	F2–F4	F2–F5	F3–F5	BL
01HTIIM88	Male	Left	59.90	77.61	109.26	50.89	68.60	100.25	49.36	406.13
01HTIIM89	Male	Right	58.37	93.62	118.64	50.71	85.96	110.98	60.27	418.83
01HTIIM162	Male	Left	59.53	96.95	118.72	49.17	86.59	108.37	59.20	422.47
01HTIIM162	Male	Right	59.82	101.21	117.82	50.91	89.88	108.91	57.99	414.28
02HTIIM178	Female	Left	45.64	75.13	103.17	39.70	69.19	97.23	57.54	375.48
02HTIIM229	Male	Left	61.98	93.52	131.49	53.06	84.60	122.57	69.51	396.52
02HTIIM229	Male	Right	59.93	90.47	116.96	51.81	82.36	108.84	57.03	392.22
02HTIIM237	Female	Left	48.22	76.13	107.97	42.61	70.52	102.36	59.76	352.90
03HTIIM245	Male	Left	66.31	95.11	124.48	60.04	88.84	118.22	58.18	416.54
03HTIIM245	Male	Right	67.09	96.71	120.14	61.97	91.59	115.01	53.04	420.19
03HTIIM266	Male	Left	58.18	88.39	120.40	48.91	79.13	111.14	62.23	396.86
03HTIIM266	Male	Right	59.41	85.04	126.53	48.42	78.42	115.55	67.12	392.24
03HTIIM290	Male	Left	62.29	92.56	113.70	55.72	92.81	107.13	51.41	420.36
03HTIIM290	Male	Right	62.24	91.58	111.12	54.87	87.05	99.67	48.87	416.29
03HTIIM300	Female	Right	49.15	87.82	107.04	41.48	78.47	99.37	57.90	373.30
03HTIIM308	Male	Left	54.73	88.08	113.13	45.34	78.70	103.74	58.40	388.65
03HTIIM315(1)	Male	Left	60.60	93.66	128.27	51.67	86.27	119.35	67.68	417.28
03HTIIM315(1)	Male	Right	57.81	88.32	122.51	48.70	79.21	113.40	64.70	412.03
03HTIIM343	Male	Left	65.46	96.78	126.95	54.13	85.45	115.62	61.49	420.17
03HTIIM346	Female	Left	55.69	87.26	120.70	47.21	78.78	112.22	65.01	371.28
03HTIIM354	Male	Right	64.23	89.33	131.52	51.95	77.05	119.24	67.29	411.13
03HTIIM357	Male	Right	58.37	94.37	117.50	50.02	84.72	109.15	59.13	390.99
03HTIIM395	Male	Left	54.94	94.58	113.80	52.63	92.27	111.49	58.86	421.13
03HTIIM395	Male	Right	59.50	93.91	127.66	53.96	88.37	122.12	68.16	417.14
03HTIIM405	Male	Right	64.80	97.28	120.14	57.77	87.45	113.12	55.35	395.28
02LJM4	Female	Left	56.51	86.28	111.26	48.30	79.35	103.06	54.75	393.50
02LJM7B	Female	Right	55.30	72.64	98.44	47.10	68.06	90.25	43.15	370.49
02LJM10	Male	Left	64.07	95.85	121.06	57.21	88.99	114.20	56.99	417.93
02LJM10	Male	Right	65.66	91.69	119.93	57.09	83.12	111.35	54.26	416.11
02LJM16	Female	Right	50.00	76.18	100.04	42.19	68.38	92.23	50.05	363.69
02LJM20	Male	Right	56.30	76.15	98.98	47.85	67.70	90.53	42.68	356.47
02LJM31B	Female	Left	53.04	78.60	97.24	46.62	72.18	90.82	44.21	353.30
03LJM41A	Female	Right	52.41	77.80	122.87	42.69	68.08	113.16	70.47	375.32
03LJM46B	Male	Right	57.87	80.13	108.26	53.38	75.64	103.76	50.38	410.01
03LJM47B	Female	Right	52.78	68.27	108.70	44.50	59.98	100.42	55.91	337.50
03LJM48	Male	Right	61.31	108.95	131.52	52.20	99.83	122.40	70.21	426.98
03LJM49A	Male	Left	58.80	96.63	143.21	53.01	90.84	137.42	84.41	405.24
03LJM49A	Male	Right	61.27	96.24	136.84	52.19	87.16	127.76	75.57	399.98
03LJM50D	Male	Left	57.10	79.53	115.43	48.40	70.83	106.73	58.33	381.56
03LJM50D	Male	Right	57.32	78.34	108.53	48.77	69.78	99.98	51.21	382.53
03LJM52A	Male	Left	64.65	101.12	115.64	56.32	92.79	107.32	50.99	410.88
03LJM53	Male	Right	64.99	98.18	120.52	56.55	89.74	112.08	55.53	410.89
03LJM54A	Female	Left	51.25	82.58	104.19	43.56	74.89	96.50	52.95	364.76
03LJM54A	Female	Right	51.85	79.56	102.93	42.92	70.63	94.00	51.08	365.26
03LJM55B	Male	Left	66.75	69.91	119.80	56.79	79.95	109.85	53.06	399.95
03LJM57A	Male	Right	54.82	81.96	114.59	44.42	71.56	104.19	59.78	366.94
99HXM2	Male	Left	64.04	108.98	124.08	56.63	89.82	116.67	60.05	406.80

(Continues)

TABLE 4 (Continued)

Specimen no.	Sex	Side	F1–F3[a]	F1–F4	F1–F5	F2–F3	F2–F4	F2–F5	F3–F5	BL
99HXM7	Male	Right	58.61	97.65	108.53	46.96	86.01	96.88	49.92	410.87
99HXM20	Male	Right	64.62	97.11	104.86	56.75	89.24	96.99	40.24	417.96
99HXM43	Male	Left	66.75	98.21	119.61	54.56	86.02	107.42	52.86	401.42
99HXM43	Male	Right	64.24	101.69	114.52	53.96	85.11	104.24	50.28	396.37
MH322	Female	Right	52.91	76.86	102.30	45.94	69.89	95.33	49.39	342.56
MH325	Female	Right	52.86	77.80	109.73	45.50	70.44	102.37	56.87	372.18
MH329	Male	Right	55.23	84.64	115.06	45.41	74.82	105.24	59.83	405.47
MH331	Female	Right	45.23	70.71	100.42	36.21	61.69	91.40	55.19	315.95
MH328	Male	Right	61.57	83.65	111.51	51.08	73.16	101.02	49.94	384.73
MH338	Female	Right	51.69	76.31	110.45	46.29	70.91	105.05	58.76	374.46
MH343	Female	Right	58.53	77.13	111.63	53.63	72.23	106.73	53.10	382.04
MH395	Female	Right	61.20	89.87	114.23	54.30	82.97	107.32	53.02	402.51

Abbreviations: BL, biomechanical length; HTIIM, Tuchengzi; HX, Xindianzi; LJ, Jinggouzi; MH, Early 20th century modern humans.
[a]Femoral segment lengths are defined by the linear distance between landmarks in Table 3, for example, F1-3 is the straight-line distance between landmark 1 and landmark 3.

biomechanical lengths (BL) of the modern Chinese samples are provided in Table 5.

Using the landmarks, we developed regression equations from the 59 recent and 20th Century modern humans (Table 2). We defined BL as the distance measured parallel to the longitudinal axis from the average distal projection of the condyles to the superior surface of the neck at its deepest point (Ruff & Hayes, 1983a). Biomechanical length was regressed on a series of segment lengths defined as distances between various pairs of landmarks on each femur (Table 4). The method for regression equations used here is classical calibration, predicting biomechanical length from segment length by regressing biomechanical length (y) on segment length (x) (Wright & Vásquez, 2003). Among equations we derived, the F2-4 regression equation was selected for use on the basis of it having the highest R^2 (0.698) and a highly significant F value (131.66, $p < 0.001$) (Table 6) that is, the F2-4 segment length is the best predictor of biomechanical length in our sample. The estimate error of each specimen was calculated by this formula that is, (|measured BL − estimated BL|)/estimated BL. The average estimate error for the reference population was calculated by dividing the sum of estimate errors by the sample size ($n = 59$). The average estimate error specifically for the F2-4 regression is equivalent to 2.71% of the estimated length. Using this approach, the Maludong femoral biomechanical length was estimated as 357.70 mm ± 2.71% (i.e., 9.71 mm), resulting in its midshaft location (50%) occurring at 178.85 ± 4.86 mm along the shaft and distal to the superior surface of the neck at its estimated deepest point.

2.4 | Acquisition of cross-sectional properties

One complete recent modern human femur was aligned in three dimensions using a standard positioning procedure following previous studies (Carlson, 2005; Ruff, 2002; Ruff & Hayes, 1983a). This procedure was performed in 3-matic (Materialize's interactive medical image control system). Subsequently, the Maludong partial femur was aligned to this reference femur by registering proximal femoral landmarks on the complete reference and the partial femur. Using our regression-based estimate of length for MLDG 1678 (i.e., 347.99–367.41 mm), intact cross sections could be identified at 65% and 80% biomechanical length (Figure 1). Both were extracted for CSG analysis. We were unable to extract an intact 50% cross section (i.e., using the regression-based estimate of length, a location between 173.99 and 183.71 mm distal to the superior surface of the neck at its deepest point) since the distalmost reasonably intact cross section observed on the partial femur was approximately 147 mm distal to the superior surface of the neck at its estimated deepest point (Figure 1). This equates to a distalmost cross section along the diaphysis available only between 57.8% and 60.0% length. Since comparative studies traditionally only include 50% or 65% diaphyseal length, without reporting CSGs from intervening areas, we chose 65% along with 80% length as a basis for comparisons.

Cross sections were imported into ImageJ 1.50e (Rasband, 2015). Standard cross-sectional properties, including subperiosteal area (TA), cortical area (CA), second moment of area (I_i), polar moment of area (J), and second moduli (Z_i), were calculated using the MomentMacroJ_v1_4B plugin (available at https://www.hopkinsmedicine.org/fae/mmacro.html). We assessed robusticity of the femoral proximal and mid-proximal diaphysis by calculating J, a measure of torsional rigidity or twice average bending rigidity.

In order to compare across individuals, we standardized J by body mass × bone length^2 (and multiplied quantities by 10^5) (Ruff, 2008; Ruff et al., 1993). Body mass of MLDG 1678 has been estimated as 50 kg (Curnoe et al., 2015). We also derived our own estimate of MLDG 1678 body mass as 58 kg based on mean body mass that was estimated from the product of anteroposterior and transverse diameters of the femoral shaft measured just inferior to the lesser trochanter (McHenry, 1992). We used this estimate in combination with our estimate of biomechanical length (347.98–367.40 mm). Percent

TABLE 5 Summary statistics for measurement lengths of the modern Chinese samples.

	Femoral length[a]	Minimum (mm)	Maximum (mm)	Mean (mm)	Standard deviation
Tuchengzi ($n = 25$)					
	F1-3	45.64	67.09	58.97	5.39
	F1-4	75.13	101.21	90.62	6.62
	F1-5	103.17	131.52	118.78	7.67
	F2-3	39.70	61.97	50.95	5.28
	F2-4	68.60	92.81	82.89	6.90
	F2-5	97.23	122.57	110.60	7.20
	F3-5	48.87	69.51	59.82	5.72
	BL	352.90	422.47	402.39	19.11
Jinggouzi ($n = 21$)					
	F1-3	50.00	66.75	57.81	5.20
	F1-4	68.27	108.95	84.60	11.14
	F1-5	97.24	143.21	114.28	12.62
	F2-3	42.19	57.21	49.62	5.28
	F2-4	59.98	99.83	77.59	10.52
	F2-5	90.25	137.42	106.10	12.56
	F3-5	42.68	84.41	56.47	10.63
	BL	337.50	426.98	386.16	25.16
Xindianzi ($n = 5$)					
	F1-3	58.61	66.75	63.65	3.02
	F1-4	97.11	108.98	100.73	4.95
	F1-5	104.86	124.08	114.32	7.85
	F2-3	46.96	56.75	53.77	4.00
	F2-4	85.11	89.82	87.24	2.13
	F2-5	96.88	116.67	104.44	8.23
	F3-5	40.24	60.05	50.67	7.11
	BL	396.37	417.96	406.68	8.35
Early 20th century modern human ($n = 8$)					
	F1-3	45.23	61.57	54.90	5.47
	F1-4	70.71	89.87	79.62	6.02
	F1-5	100.42	115.06	109.42	5.31
	F2-3	36.21	54.30	47.30	5.81
	F2-4	61.69	82.97	72.01	5.90
	F2-5	91.40	107.32	101.81	5.71
	F3-5	49.39	59.83	54.51	3.85
	BL	351.95	405.47	327.49	30.06

[a]Femoral segment lengths are defined by the linear distance between landmarks in Table 3, for example, F1-3 is the straight-line distance between landmark 1 and landmark 3.

cortical area [%CA, (CA/TA) × 100] reflects the balance of endosteal resorption and subperiosteal deposition through an individual's life (Ruff, 2008; Ruff et al., 1994; Ruff & Hayes, 1983b). We also compared a rigidity index (I_x/I_y) and shape index (I_{max}/I_{min}) of MLDG 1678 to indices from all Pleistocene samples. Statistical analyses were performed using SPSS 20.0 statistical software (SPSS Inc., Chicago, IL). The nonparametric Kruskal–Wallis test was chosen to evaluate group differences in standardized J, %CA, and diaphyseal indices. Statistical significance used an alpha value of 0.05 ($p < 0.05$).

3 | RESULTS

3.1 | Femoral diaphyseal robusticity

Unstandardized cross-sectional geometric properties of MLDG 1678 are provided in Table 7. When standardizing properties for comparisons, there are no significant group differences in standardized J at the mid-proximal location ($H = 5.013$, df $= 4$, $p = 0.286$), while there are significant group differences in the subtrochanteric region ($H =$

TABLE 6 Linear regression equations for estimates of femoral biomechanical length.

Linear regression equation	R^2[a]	Adjust R^2	F	Sig. (p)[b]	SE[c]
BL = 193.119 + 3.421 × (F1-3)	0.572	0.564	76.15	<0.001	16.33
BL = 226.295 + 1.897 × (F1-4)	0.574	0.567	76.90	<0.001	16.29
BL = 217.267 + 1.520 × (F1-5)	0.367	0.356	33.10	<0.001	19.85
BL = 217.438 + 3.494 × (F2-3)	0.577	0.569	77.69	<0.001	16.24
BL = 209.875 + 2.291 × (F2-4)	0.698	0.693	131.66	<0.001	13.72
BL = 228.392 + 1.534 × (F2-5)	0.363	0.352	32.51	<0.001	32.51
BL = 353.255 + 0.694 × (F3-5)	0.052	0.035	3.11	0.083	24.31

[a]Coefficient of determination.
[b]Sig., significance.
[c]SE, standard error of the estimate.

TABLE 7 Unstandardized cross-sectional geometric properties of the Maludong femur.

Cross-sectional properties	65%[a]	80%[a]
Total area (TA)	373.7–382.2	421.0–443.5
Cortical area (CA)	261.2–264.3	268.1–276.4
Percent cortical area (%CA)[b]	**69.0–70.3**	**62.3-64.1**
Anteroposterior second moment of area (I_x)	13301.9–13641.3	12924.3–13797.4
Mediolateral second moment of area (I_y)	8029.9–8392.7	12699.6–12903.7
Diaphyseal index (I_x/I_y)[b]	**1.62–1.66**	**0.97-1.02**
Maximum second moment of area (I_{max})	13651.5–14088.6	16543.2–17696.4
Minimum second moment of area (I_{min})	7680.3–7945.5	9169.3–10061.4
I_{max}/I_{min}	**1.76–1.78**	**1.79–1.80**
Polar moment of area (J)[b]	**21331.8–22034.1**	**25712.5-28030.7**
Anteroposterior section modulus (Z_x)	993.3–1016.5	1050.4–1106.6
Mediolateral section modulus (Z_y)	829.1–865.2	1043.7–1050.4
Polar section modulus (Z_p)	1597.2–1632.9	1840.2–1982.9

[a]Using the estimated biomechanical length (i.e., 347.99–367.41 mm) of Maludong femur in this study, there are variation ranges of locations for both 65% and 80% cross sections, see Figure 1. Here, we report a range of cross-sectional geometric properties calculated with respect to location variations of 65% and 80%.
[b]Bold font indicates indices for comparison.

17.145, df = 4, p = 0.002). Notably, the MPMH and E/MUP groups are significantly lower than the Neandertal sample (p = 0.026 and 0.004, respectively) at the subtrochanteric location (Figure 2b). Visual comparisons of standardized J also revealed that EMP and Neandertal samples tended to exhibit higher median robusticity than EP (KNM-ER 1472, KNM-ER 1481a) and early modern human samples, although overlap in group ranges was observed (Figure 2a). MLDG 1678 was lower than the median values of standardized J for all comparative groups, and fits into the bottom of the range for E/MUP and MPMH group (Figure 2a). Standardized J of the East Asian early modern human Tianyuan 1 femoral cross sections (65%: 509.4 for right PA1290 and 461.4 for left PA1289; 80%: 549.0 for right PA1290 and 493.2 for left PA1289) were higher than those of the Maludong femoral cross sections (65%: 314.5–324.8, 80%: 379.0–413.2) (Figure 2a,b).

When comparing %CA, no significant group differences were observed in either of the mid-proximal or subtrochanteric regions (65%: H = 7.201, df = 6, p = 0.303; 80%: H = 1.669, df = 6, p = 0.947). The Maludong femur (65%: 69.0–70.3) was consistently markedly lower than group medians, and even below the non-extreme outliers exhibited by EP, LMP, Neanderthal, MPMH and East Asian LUP (only Maomaodong) groups (Figure 2b). Comparisons of the Maludong subtrochanteric region (80%: 62.3–64.1) indicated similar results in that its %CA was consistently lower than group medians, although in this location the Maludong femur fell entirely below ranges of variation exhibited by EP, EMP, MPMH, and E/MUP groups (Figure 2b). By comparison, %CA of other LPMH femora from the region that is, Tianyuan 1 (65%: 86.2 for right PA1290 and 82.7 for left PA1289; 80%: 84.7 for right PA1290 and 82.2 for left PA1289) and Maomaodong (65%: 86.3 for GM7506 and 79.4 for GM7508; 81.1 for GM7508) tended to fall at the upper end of ranges of variation in the comparative groups (Figure 2a,b).

3.2 | Femoral diaphyseal ratio

Comparisons of MLDG 1678 ratios of anteroposterior vs. mediolateral second moments of area (I_x/I_y) and maximum vs minimum second

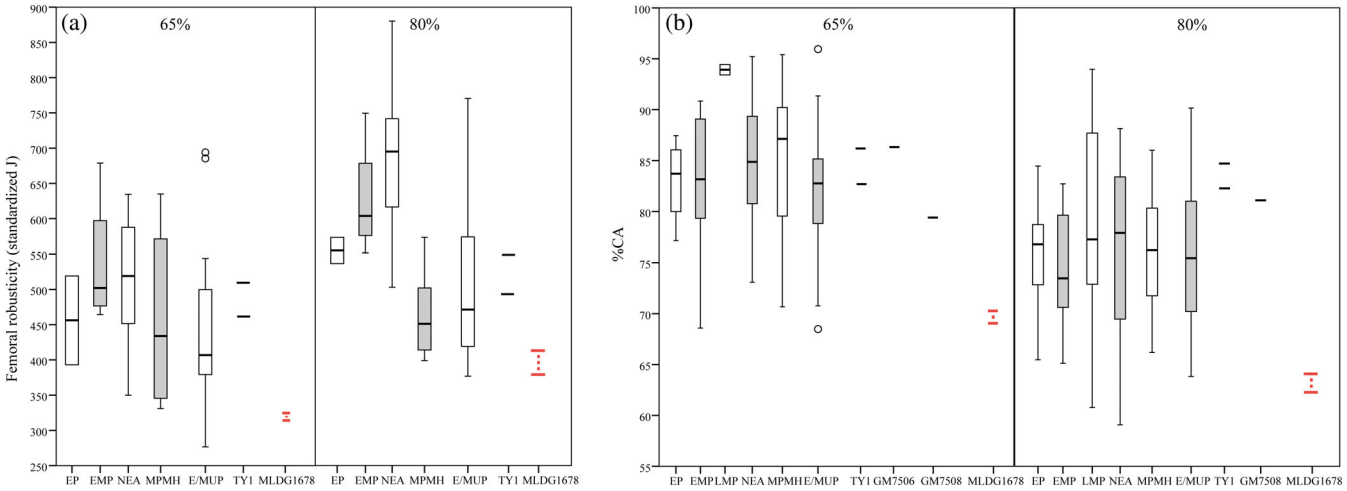

FIGURE 2 Box plots of femoral mid-proximal and subtrochanteric diaphyseal robusticity. (a: Femoral robusticity (standardized *J*)) as measured by standardized polar moment of area, *J*, for MLDG 1678 and comparative samples. Box plot of percent cortical area (b: %CA) for MLDG 1678 and comparative samples from the same diaphyseal locations. Polar moment of area standardized by the product of body mass and squared biomechanical length. The solid horizontal red lines in comparisons of standardized polar moments of area indicate the range of values for the Maludong femur incorporating average error estimates of length. Boxplots indicate the median (horizontal bar), upper and lower quartile (boxes), and upper and lower outlier non-extreme values (vertical bar). E/MUP, Early and Middle Upper Paleolithic modern humans; EMP, Early Middle Pleistocene; EP, Early Pleistocene; MPMH, Middle Paleolithic modern humans; NEA, Neandertals; TY1, Tianyuan 1 femora; and Maomaodong femora (GM 7506 and GM 7508)

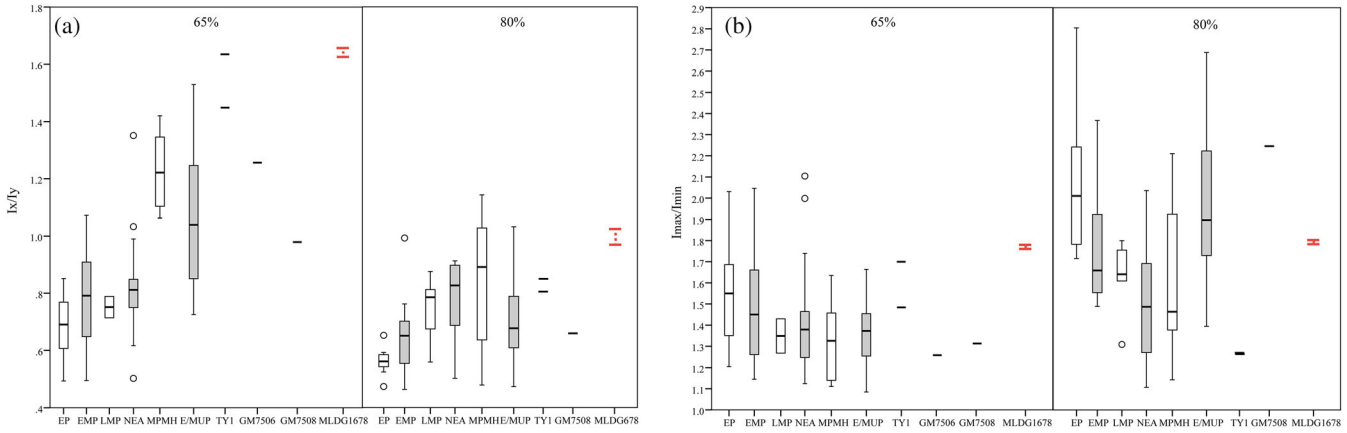

FIGURE 3 Box plots of femoral mid-proximal (65%) and subtrochanteric (80%) anteroposterior vs. mediolateral (a: I_x/I_y) and maximum vs minimum (b: I_{max}/I_{min}) second moments of area for MLDG 1678 and comparative samples. The solid horizontal red lines in comparisons of indicate the values for the Maludong femur that incorporate 5° clockwise and counterclockwise rotations of neutral axes. Boxplots indicate the median (horizontal bar), upper and lower quartile (boxes), and upper and lower outlier non-extreme values (vertical bar). E/MUP, Early and Middle Upper Paleolithic modern human; EMP, Early Middle Pleistocene; EP, Early Pleistocene; MPMH, Middle Paleolithic modern humans; NEA, Neandertals; TY1, Tianyuan 1 femora; and Maomaodong femora (GM 7506 and GM 7508)

moments of area (I_{max}/I_{min}) showed contrasting trends when evaluated against the comparative sample, especially at the mid-proximal location (Figure 3a). In ratios of I_x/I_y, there are significant group differences among the comparative samples (65%: $H = 34.141$, df = 6, $p < 0.001$; 80%: $H = 15.894$, df = 6, $p = 0.014$). At the mid-proximal cross section, the Late Pleistocene modern human (LPMH, 11,700–126,000 BP) samples exhibited a significantly higher I_x/I_y ratio than the EP ($p = 0.003$ for both MPMH and E/MUP), EMP ($p = 0.018$ for MPMH and $p = 0.020$ for E/MUP), and Neandertal ($p = 0.033$ for MPMH and $p = 0.029$ for E/MUP) groups (Figure 3a), suggesting relatively greater anteroposterior rigidity in the former. The MLDG 1678 femur also exhibited a ratio favoring anteroposterior rigidity at this diaphyseal location ($I_x/I_y = 1.62–1.66$), being substantially higher than those of all comparative groups, and falling only within the upper end of the range of variation observed in the LPMH. Interestingly, the Maludong femur is intermediate in this ratio to those of the Tianyuan 1 individual (right PA1290 = 1.45 and left PA1289 = 1.63). At the subtrochanteric region, the EP sample was significantly lower than the

Neandertal ($p = 0.015$) sample (Figure 3a), exhibiting the relatively greatest mediolateral rigidity. Although the degree to which MLDG 1678 tended to exceed other group ranges was not as marked in the subtrochanteric region as in the mid-proximal region, it still fell almost exclusively within the upper range of variation observed in the LPMH and close to exhibiting equivalent anteroposterior and mediolateral rigidities. The subtrochanteric region of Maludong (0.97–1.02) is higher in its I_x/I_y rigidity ratio than either of the Tianyuan 1 femora (right PA1290 = 0.80 and left PA1289 = 0.85) or the Maomaodong femur (GM7508 = 0.66) that preserved this region (Figure 3a).

In evaluating diaphyseal shape ratios, the general trend was either consistency in ratios across groups (65%: $H = 3.844$, df = 5, $p = 0.572$) or a general decrease from the earlier groups to the later groups (80%), with the exception of the LPMH groups. While little separation between groups was observed in the I_{max}/I_{min} ratio at 65% locations, the Maludong femur still exhibited a relatively higher value (i.e., more elliptical shape) than a majority of the comparative groups (Figure 3b). At the subtrochanteric region (80%), on the other hand, there were significant group differences among the comparative samples ($H = 18.380$, df = 5, $p = 0.003$). The Neandertal sample was significantly lower than the EP ($p = 0.019$) and E/MUP ($p = 0.009$) samples. The shape ratio of the subtrochanteric region of the Maludong femur (MLDG 1678) overlapped more comfortably within the range of variation (i.e., within quartiles) of the EP, EMP, MPMH and E/MUP groups than within the lower (i.e., less elliptical) LMP and Neanderthal samples (Figure 3 B). Tianyuan 1 femora exhibited subtrochanteric shape ratios (right PA1290 = 1.27 and left PA1289 = 1.26) that were substantially lower than the Maludong (1.79–1.80) and Maomaodong (GM7508 = 2.25) shape ratios. In fact, combining values from the three sites (Tianyuan 1, Maomaodong, and Maludong) would approximate the range of variability exhibited by the EP group and exceed other group ranges of variability except for the highly variable LPMH groups (Figure 3b).

4 | DISCUSSIONS AND CONCLUSION

For femoral robusticity represented by scaled polar moments of area, MLDG 1678 is within the range of variation of multiple groups of Pleistocene hominins, indicating a level of femoral robusticity commensurate with mobility that characterized Pleistocene foraging populations, especially the LPMH that is, MPMH, E/MUP, and East Asian LUP group. The I_{max}/I_{min} subtrochanteric ratio and I_x/I_y ratios at mid-proximal and subtrochanteric locations exhibited significant differences among the comparative samples. By combining the two ratios, relative rigidities can be more fully understood. The MLDG 1678 femur is within the range of shape variation of multiple groups of Pleistocene hominins, although its mid-proximal location is near the upper end in its ellipticity. Comparing I_x/I_y ratios, the Maludong femoral mid-proximal cross section is again confirmed as relatively distinctive, exhibiting markedly greater anteroposterior rigidity similar to LPMH femora, including MPMH, E/MUP, and East Asian LUP groups. Thus, greater ellipticity in the mid-proximal diaphysis of MLDG 1678 appears to reflect its relatively greater rigidity in an anteroposterior plane.

It is unclear whether the trend favoring relative anteroposterior diaphyseal rigidity in MLDG 1678 would have been more or less apparent, if regions of the diaphysis distal to 57%–60% length were preserved. If the midshaft was preserved, as others have proposed (Curnoe et al., 2015), biomechanical length of the MLDG femur would have been approximately 294 mm for this distalmost intact cross section to coincide with a midshaft location. Our regression-derived estimate of 347.98–367.40 mm (18%–25% greater than 294 mm) emphasizes how unlikely it is that the midshaft location is preserved on the remaining portion of the MLDG 1678 partial femur. Nonetheless, even substituting a maximum length with respect to the remaining anterior portion of the uneven distal break (and assuming the previous study filled in missing areas of the cross section), thus considering 167 mm as the midshaft location, the resulting biomechanical length (334 mm) would still be 14 mm shorter than our regression-derived minimum estimate (348 mm). Thus, it is unlikely that the midshaft region is preserved on this specimen, ultimately making midshaft comparisons with other femora implausible.

Among the external features that align MLDG 1678 with more archaic than modern humans (Curnoe et al., 2015), several are worth further consideration. Low neck-shaft angle is not necessarily an exclusively archaic-like feature since it also is exhibited by Early/Middle Upper Paleolithic femora from Europe (Trinkaus, 2015). Damage on the Maludong femoral neck and a missing femoral head (Figure 1) suggests any measurement of its biomechanical neck length should be considered with extreme caution. Since it appears that the Maludong femur is broken proximal to midshaft, we also suggest assessment of a femoral pilaster should be considered with caution. Additionally, the remaining proximal shaft of MLDG 1678 hints at a developed linea aspera and a prominent pilaster on its posterior aspect, which are typical features in early modern human rather than archaic femora (Trinkaus & Ruff, 2012).In sum, detailed structural analysis of the Maludong femoral diaphysis demonstrates that its internal features are within the range of variation of those observed in other Late Pleistocene humans. Discrepancies with outcomes based on external character comparisons could benefit from further scrutiny of the external configuration of the Maludong femur. Based on our analysis of internal structure of the Maludong femur, there is no support for a potential second 'population' in the region characterized by more archaic postcranial morphology. Rather, the present analysis of internal structure suggests that the Maludong femur expands the extent of postcranial intrapopulation variability that has been documented in modern human-like populations of East Asia such as those represented postcranially by material from Zhaoguo and Maomaodong (Wei et al., 2020; Wei, Weng, et al., 2021).

AUTHOR CONTRIBUTIONS

Pianpian Wei: Data curation (equal); formal analysis (lead); funding acquisition (lead); methodology (lead); project administration (equal); writing – original draft (lead). **Shiwu Ma:** Data curation (lead); resources (lead). **Xueping Ji:** Data curation (equal); resources (equal).

Quanchao Zhang: Data curation (equal); resources (equal). **Wu Liu:** Funding acquisition (lead); methodology (equal). **Li Jin:** Funding acquisition (lead); supervision (lead). **Kristian Carlson:** Data curation (equal), formal analysis (equal), methodology (lead), writing - original draft (lead).

ACKNOWLEDGMENTS

This work was supported by the Strategic Priority Research Program of the Chinese Academy of Sciences (XDB26000000), the National Natural Science Foundation of China (41802020), the China Postdoctoral Science Foundation (2017M611449), the Key projects of strategic international scientific and technological innovation cooperation of the Chinese Ministry of Science and Technology (2020YFE0201600), the Scientific and Technology Committee of Shanghai Municipality (18490750300), and 111 Project (B13016).

CONFLICT OF INTEREST

The authors declare no conflict of interest.

DATA AVAILABILITY STATEMENT

All data that support this study are published in this manuscript.

ORCID

Pianpian Wei https://orcid.org/0000-0001-7815-1675
Kristian J. Carlson https://orcid.org/0000-0001-5802-9680
Wu Liu https://orcid.org/0000-0002-8444-368X

REFERENCES

Carlson, K. J. (2005). Investigating the form-function interface in African apes: Relationships between principal moments of area and positional behaviors in femoral and humeral diaphyses. *American Journal of Physical Anthropology*, *127*(3), 312–334. https://doi.org/10.1002/ajpa.20124

Carlson, K. J., & Marchi, D. (2014). Reconstructing mobility: Enviromental, behavioral, and morphological determinants. In *Reconstructing mobility*. Springer. https://doi.org/10.1007/978-1-4899-7460-0

Chevalier, T., Özçelik, K., De Lumley, M.-A., Kösem, B., De Lumley, H., Yalçinkaya, I., & Taşkiran, H. (2015). The endostructural pattern of a middle pleistocene human femoral diaphysis from the Karain E site (southern Anatolia, Turkey). *American Journal of Physical Anthropology*, *157*(4), 648–658. https://doi.org/10.1002/ajpa.22762

Curnoe, D., Ji, X., Liu, W., Bao, Z., Taçon, P. S. C., & Ren, L. (2015). A hominin femur with archaic affinities from the late Pleistocene of Southwest China. *PLoS One*, *10*, e0143332. https://doi.org/10.1371/journal.pone.0143332

McHenry, H. M. (1992). Body size and proportions in early hominids. *American Journal of Physical Anthropology*, *87*(4), 407–431. https://doi.org/10.1002/ajpa.1330870404

Puymerail, L., Ruff, C. B., Bondioli, L., Widianto, H., Trinkaus, E., & Macchiarelli, R. (2012). Structural analysis of the Kresna 11 Homo erectus femoral shaft (Sangiran, Java). *Journal of Human Evolution*, *63*(5), 741–749. https://doi.org/10.1016/j.jhevol.2012.08.003

Rasband, W. S. (2015). *ImageJ*. National Institute of Health.

Rodríguez, L., Carretero, J. M., García-González, R., & Arsuaga, J. L. (2018). Cross-sectional properties of the lower limb long bones in the middle Pleistocene Sima de los Huesos sample (sierra de Atapuerca, Spain). *Journal of Human Evolution*, *117*, 1–12. https://doi.org/10.1016/j.jhevol.2017.11.007

Ruff, C. B. (2002). Long bone articular and diaphyseal structure in old world monkeys and apes. I: Locomotor effects. *American Journal of Physical Anthropology*, *119*(4), 305–342. https://doi.org/10.1002/ajpa.10117

Ruff, C. B. (2008). Biomechanical analyses of archaeological human skeletons. In M. A. Katzenberg & S. R. Saunders (Eds.), *Biological anthropology of the human skeleton* (2nd ed., pp. 183–206). John Wiley & Sons, Inc.. https://doi.org/10.1002/9780470245842

Ruff, C. B. (2009). Relative limb strength and locomotion in *Homo habilis*. *American Journal of Physical Anthropology*, *138*, 90–100.

Ruff, C. B., & Hayes, W. (1983a). Cross-sectional geometry of Pecos Pueblo femora and tibiae—A biomechanical investigation: I. Method and general patterns of variation. *American Journal of Physical Anthropology*, *60*, 359–381. https://doi.org/10.1002/ajpa.1330600308

Ruff, C. B., & Hayes, W. C. (1983b). Cross-sectional geometry of Pecos Pueblo femora and tibiae-a biomechanical investigation: II. Sex, age and side differences. *American Journal of Physical Anthropology*, *60*, 383–400.

Ruff, C. B., Holt, B., Niskanen, M., Sládek, V., Berner, M., Garofalo, E., Garvin, H. M., Hora, M., Junno, J. A., Schuplerova, E., Vilkama, R., & Whittey, E. (2015). Gradual decline in mobility with the adoption of food production in Europe. *Proceedings of the National Academy of Sciences of the United States of America*, *112*(23), 7147–7152. https://doi.org/10.1073/pnas.1502932112

Ruff, C. B., Holt, B., & Trinkaus, E. (2006). Who's afraid of the big bad Wolff? "Wolff's law" and bone functional adaptation. *American Journal of Physical Anthropology*, *129*(4), 484–498. https://doi.org/10.1002/ajpa.20371

Ruff, C. B., Holt, B. M., Sládek, V., Berner, M., Murphy, W. A., Jr., zur Nedden, D., Seidler, H., & Recheis, W. (2006). Body size, body proportions, and mobility in the Tyrolean "'iceman". *Journal of Human Evolution*, *51*, 91–101. https://doi.org/10.1016/j.jhevol.2006.02.001

Ruff, C. B., Larsen, C. S., & Hayes, W. C. (1984). Structural changes in the femur with the transition to agriculture on the Georgia coast. *American Journal of Physical Anthropology*, *64*, 125–136. https://doi.org/10.1002/ajpa.1330640205

Ruff, C. B., Puymerail, L., Macchiarelli, R., Sipla, J., & Ciochon, R. L. (2015). Structure and composition of the Trinil femora: Functional and taxonomic implications. *Journal of Human Evolution*, *80*, 147–158. https://doi.org/10.1016/j.jhevol.2014.12.004

Ruff, C. B., Trinkaus, E., Walker, A., & Larsen, C. S. (1993). Postcranial robusticity in *Homo*. I: Temporal trends and mechanical interpretation. *American Journal of Physical Anthropology*, *91*(1), 21–53. https://doi.org/10.1002/ajpa.1330910103

Ruff, C. B., Walker, A., & Trinkaus, E. (1994). Postcranial robusticity in *Homo*. III: Ontogeny. *American Journal of Physical Anthropology*, *93*, 35–54.

Shackelford, L. L. (2007). Regional variation in the postcranial robusticity of late upper paleolithic humans. *American Journal of Physical Anthropology*, *133*(1), 655–668. https://doi.org/10.1002/ajpa.20567

Shang, H., & Trinkaus, E. (2010). *The early modern human from Tianyuan cave, China* (pp. 96–131). Texas A&M University Press.

Stock, J. T., & Macintosh, A. A. (2016). Lower limb biomechanics and habitual mobility among mid-Holocene populations of the cis-Baikal. *Quaternary International*, *405*, 200–209. https://doi.org/10.1016/j.quaint.2015.04.052

Stock, J. T., & Pfeiffer, S. K. (2004). Long bone robusticity and subsistence behaviour among later stone age foragers of the forest and fynbos biomes of South Africa. *Journal of Archaeological Science*, *31*(7), 999–1013. https://doi.org/10.1016/j.jas.2003.12.012

Trinkaus, E. (2015). The appendicular skeletal remains of Oberkassel 1 and 2. In L. Giemsch & R. W. Schmitz (Eds.), *The last glacial burial from Oberkassel revisited* (pp. 75–132). Verlag Phillip von Zabern.

Trinkaus, E., & Ruff, C. B. (1999). Diaphyseal cross-sectional geometry of near eastern middle Paleolithic humans: The femur. *Journal of Archaeological Science*, *26*, 409–424.

Trinkaus, E., & Ruff, C. B. (2012). Femoral and tibial diaphyseal cross-sectional geometry in Pleistocene homo. *PaleoAnthropology*, 13–62. https://doi.org/10.4207/PA.2012.ART69

Wang, Y., Wei, C., Que, J., Zhang, W., Sun, C., Shu, Y., Hou, Y. M., Zhang, J. C., Shi, R. J., & Wei, L. (2019). Development and applications of paleontological computed tomography. *Vertebrata PalAsiatica*, *57*(1), 84–92. https://doi.org/10.19615/j.cnki.1000-3118.170921

Wei, P., Lu, H., Carlson, K. J., Zhang, H., Hui, J., Zhu, M., He, K., Jashashvili, T., Zhang, X., Yuan, H., & Xing, S. (2020). The upper limb skeleton and behavioral lateralization of modern humans from Zhaoguo cave, southwestern China. *American Journal of Physical Anthropology*, *173*(4), 671–696. https://doi.org/10.1002/ajpa.24147

Wei, P., Wallace, I. J., Jashashvili, T., Musiba, C. M., & Liu, W. (2017). Structural analysis of the femoral diaphyses of an early modern human from Tianyuan cave, China. *Quaternary International*, *434*, 48–56. https://doi.org/10.1016/J.QUAINT.2015.10.099

Wei, P., Weng, Z., Carlson, K. J., Cao, B., Jin, L., & Liu, W. (2021). Late Pleistocene partial femora from Maomaodong, southwestern China. *Journal of Human Evolution*, *155*, 102977. https://doi.org/10.1016/j.jhevol.2021.102977

Wei, P., Zhao, Y., Walker, C. S., He, J., & Lu, X. (2021). Internal structural properties of the humeral diaphyses in an early modern human from Tianyuan cave, China. *Quaternary International*, *591*, 107–118. https://doi.org/10.1016/j.quaint.2021.04.012

Wright, L. E., & Vásquez, M. A. (2003). Estimating the length of incomplete long bones: Forensic standards from Guatemala. *American Journal of Physical Anthropology*, *120*(3), 233–251. https://doi.org/10.1002/ajpa.10119

Zhang, X., Zheng, L., Yang, L., & Bao, Z. (1990). The human fossils and the palaeoculture from Mengzi, Yunnan province. *Social Sciences in Yunnan*, *2*, 60–64.

How to cite this article: Wei, P., Ma, S., Carlson, K. J., Ji, X., Zhang, Q., Liu, W., & Jin, L. (2022). A structural reassessment of the Late Pleistocene femur from Maludong, southwestern China. *American Journal of Biological Anthropology*, *178*(4), 655–666. https://doi.org/10.1002/ajpa.24569